Journal of Thermal Analysis and Calorimetry, Vol. 91 (2008) 2, 525–528

THERMAL BEHAVIOUR AND FRAGILITY OF Sb_2O_3-CONTAINING ZINC BOROPHOSPHATE GLASSES

J. Šubčík, P. Mošner and L. Koudelka[*]

Department of General and Inorganic Chemistry, Faculty of Chemical Technology, University of Pardubice
53210 Pardubice, Czech Republic

Thermal behaviour of the glass series $(100–x)[50ZnO–10B_2O_3–40P_2O_5]\cdot xSb_2O_3$ (x=0–42 mol%) and $(100–y)[60ZnO–10B_2O_3–30P_2O_5]\cdot ySb_2O_3$ (y=0–28 mol%) was investigated by DSC and TMA. The addition of Sb_2O_3 results in a decrease of the glass transition temperature and crystallization temperature in both compositional series. All glasses crystallize on heating in the temperature range of 522–632°C. Thermal expansion coefficient of the glasses monotonously increases with increasing Sb_2O_3 content in both series and varies within the range of 6.6–11.7 ppm $°C^{-1}$. From changes of thermal capacity within the glass transition region it was concluded that with increasing Sb_2O_3 content the 'fragility' of the studied glasses increases.

Keywords: *antimony oxide, borophosphate glasses, DSC, fragility, glass-forming tendency*

Introduction

Phosphate and borophosphate glasses have been studied in recent years for various technological applications [1]. One of them is for glass-to-metal seals due to their low melting temperature and low viscosity. Borophosphate glasses reveal higher chemical durability than phosphate glasses due to the incorporation of boron oxide into the structural network, mostly in the form of BO_4 tetrahedra, which transform metaphosphate chains into three-dimensional network [3]. Zinc borophosphate glasses were studied in several papers [3–6]. Glass-forming region in the $ZnO–B_2O_3–P_2O_5$ ternary system was published in 1975 by Ushakov *et al.* [3]. Clinton and Coffeen [4] studied zinc borophosphate glasses for the application as packaging and enameling solder glasses and Brow and Tallant [2] for seals in flat panel displays. Structure of zinc borophosphate glasses in the compositional series of $xB_2O_3(1–x)Zn(PO_3)_2$ was studied by Brow [5] using XPS and ^{11}B MAS NMR. By curve fitting of O1s spectra he obtained the relative concentrations of P–O–P, P–O–Zn and P–O–B bonds in these glasses. Brow and Tallant [2] studied the structure of $Zn(PO_3)_2–B_2O_3$ and $Zn_2P_2O_7–B_2O_3$ glasses with ^{31}P and ^{11}B MAS NMR technique and Raman spectroscopy. From these studies they proposed a model of the evolution of glass structure from phosphate to borophosphate network. The relations between structure and physical properties of glasses within $ZnO–B_2O_3–P_2O_5$ ternary system were studied in [6] within several different compositional series. Kinetics and mechanism of crystallization of zinc borophosphate glasses was studied in [7] by thermal analysis and X-ray diffraction. Zinc borophosphate glasses after crystallization give at least 2 crystalline products. One of them is BPO_4 and the other is a zinc phosphate, the composition of which depends on the ratio of Zn/P in the sample after the formation of BPO_4.

The doping of zinc borophosphate glasses with other oxides, which are able to enter glass network, can retain the relatively good chemical durability of borophosphate glasses and modify their properties [8, 9]. Doping of borophosphate glasses with antimony oxide [10] showed that the borophosphate network is able to incorporate a relatively high content of this intermediary oxide. This paper deals with the preparation and study of the effect of Sb_2O_3 on the thermal behaviour and crystallization of zinc borophosphate glasses in two compositional series.

Experimental

Glasses of series $(100–x)[50ZnO–10B_2O_3–40P_2O_5]\cdot xSb_2O_3$ and $(100–y)[60ZnO–10B_2O_3–30P_2O_5]\cdot ySb_2O_3$ were prepared from reagent grade ZnO, H_3BO_3, H_3PO_4 and Sb_2O_3 in batches of 20 g. In the first stage the reaction mixture was heated slowly in a platinum crucible up to 600°C with the final calcination at the maximum temperature for 2 h to remove water. After the calcination the reaction mixture was heated slowly up to 1200–1280°C. After 20 min heating at the maximum temperature, the obtained melt was cooled by pouring

* Author for correspondence: ladislav.koudelka@upce.cz

1388–6150/$20.00

Akadémiai Kiadó, Budapest, Hungary
Springer, Dordrecht, The Netherlands

into a graphite mould of 30x30 mm dimensions to form a suitable glass block. The obtained glasses were separately annealed for 15 min at a temperature close to their T_g and then slowly cooled to room temperature.

Thermal behaviour of the glasses was studied with the Netzsch DTA 404 PC equipment in the DSC mode in the temperature range of 20–1000°C at the heating rate of 10°C min^{-1}. For these measurements glassy samples were powdered in a vibrational mill with the corundum lining for 30 s. The measured samples were placed in silica crucibles. Dilatation curves of the studied glasses were measured on the equipment TMA CX04R to obtain glass transition temperature, dilatation softening temperature and the thermal expansion coefficients. These measurements were carried out at the heating rate of 10°C min^{-1}. For these measurements the cubes of 5×5×5 mm were cut out from glass blocks.

Results and discussion

In the first series (100–x)[50ZnO–10B_2O_3–40P_2O_5]·$x$$Sb_2O_3$ under the slow cooling the melt homogeneous glasses were obtained within the compositional region of x=0–42 mol% Sb_2O_3, whereas in the second compositional region (100–y)[60ZnO–10B_2O_3–30P_2O_5]·$y$$Sb_2O_3$ homogeneous glasses were obtained only within the compositional region of y=0–28 mol% Sb_2O_3. All the obtained glasses were transparent and their glassy state was checked by X-ray diffraction analysis. Thermal analysis of ZnO–B_2O_3–P_2O_5–Sb_2O_3 glasses was carried out with powder samples of mean particle size ≈8 μm. Figures 1a and 1b show DSC curves of glass samples from the compositional series (100–x)[50ZnO–10B_2O_3–40P_2O_5]·$x$$Sb_2O_3$, where x=0–42 mol% Sb_2O_3. Figure 2 shows DSC curves of glass samples from the compositional series (100–y)[60ZnO–10B_2O_3–30P_2O_5]·$y$$Sb_2O_3$, where x=0–28 mol% Sb_2O_3. From the obtained DSC curves we determined the values of the glass transition temperature, T_g (determined as the midpoint of the change in C_p) and the crystallization temperature, T_c, (determined as the onset of the first crystallization peak) using the software 'Proteus Analysis' supplied with the equipment.

The obtained compositional dependence of glass transition temperature for the glasses of the first series (100–x)[50ZnO–10B_2O_3–40P_2O_5]·$x$$Sb_2O_3$ is shown in Fig. 3. As can be seen T_g values in this glass series decrease with increasing Sb_2O_3 content from 479°C for the undoped glass 50ZnO–10B_2O_3–40P_2O_5 down to 391°C for the glass 58[50ZnO–10B_2O_3–40P_2O_5]·42Sb_2O_3. As the structural studies [8] showed that antimony oxide enters structural network in the form of SbO_3 pyramids, which is accompanied by the depolymerization of phosphate chains and formation of Sb–O–P bonds, we can conclude that this process results in a decrease of bonding strength inside the network reflected by the observed decrease in the glass transition temperature with increasing Sb_2O_3 content. Similar trend in T_g values we can see in the glasses of the second compositional series (100–y)[60ZnO–10B_2O_3–30P_2O_5]·$y$$Sb_2O_3$ (Fig. 4), where T_g decreases from 477°C, for the undoped glass 60ZnO–10B_2O_3–30P_2O_5, down to 421°C for the glass with y=28.6 mol% Sb_2O_3.

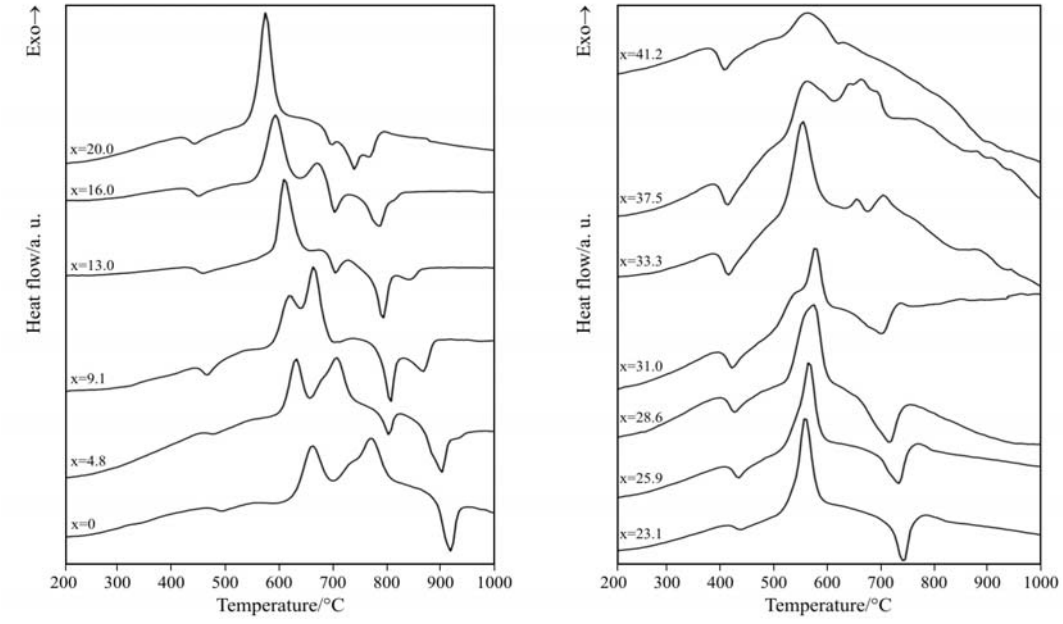

Fig. 1 DSC curves of glass series (100–x)[50ZnO–10B_2O_3–40P_2O_5]·$x$$Sb_2O_3$

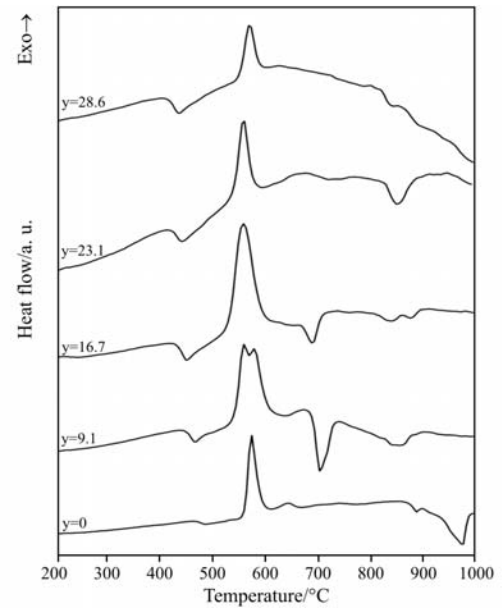

Fig. 2 DSC curves of glass series $(100–y)[60ZnO–10B_2O_3–30P_2O_5]·ySb_2O_3$

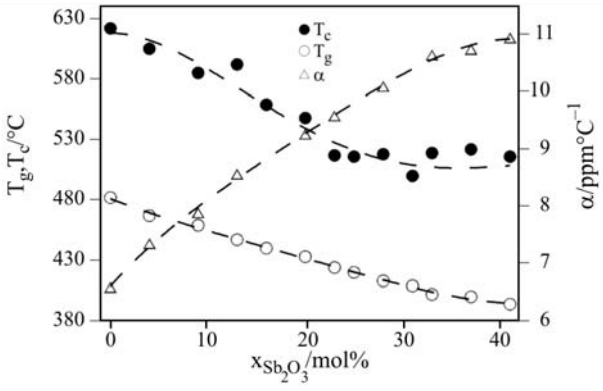

Fig. 3 Glass transition temperature, crystallization temperature and thermal expansion coefficient of $(100–x)[50ZnO–10B_2O_3–40P_2O_5]·xSb_2O_3$ glasses

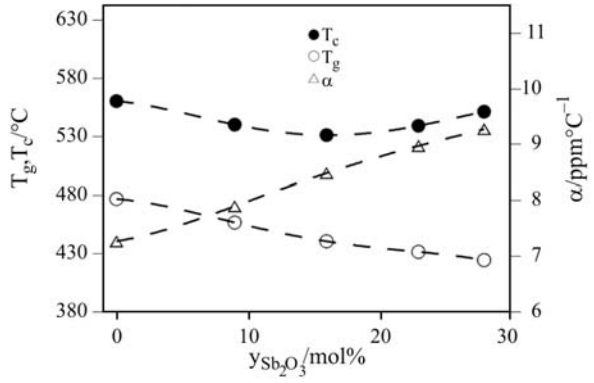

Fig. 4 Glass transition temperature, crystallization temperature and thermal expansion coefficient of $(100–y)[60ZnO–10B_2O_3–30P_2O_5]·ySb_2O_3$ glasses

On the DSC curves of the studied glasses we have observed also that with increasing Sb_2O_3 content the change in C_p in the glass transition region increases (Fig. 1). The values of ΔC_p (in J mol^{-1} °C^{-1}) were obtained from measured ΔC_p (in J g^{-1} °C^{-1}) values by multiplication with molecular mass calculated as

$$M=[xM(Sb_2O_3)+(100–x)(0.5M(ZnO)+ 0.1M(B_2O_3)+0.4M(P_2O_5))]/100 \quad [g\ mol^{-1}]$$

The heat capacity changes, $\Delta C_p=C_{pl}–C_{pg}$ (C_{pl} is the heat capacity in the liquid-state and C_{pg} is the heat capacity of the glassy state) in the glass transition region were found to be independent of the heating rate. The values of ΔC_p for the $(100–x)[50ZnO–10B_2O_3–40P_2O_5]·xSb_2O_3$ glasses as a function of Sb_2O_3 content are shown in Fig. 5. From this figure it is evident that ΔC_p values steeply increase with Sb_2O_3 content from 2.8 (x=0) to 17.8 J mol^{-1} °C^{-1} (x=33.33). A correlation between ΔC_p and fragility characteristic is not so straightforward like the correlation between the fragility and the ratio C_{pl}/C_{pg}, but strong liquids usually show smaller changes of ΔC_p in the glass transition region than the fragile liquids [11]. From this point of view, the observed ΔC_p changes (Fig. 5) indicate that the fragility of the $(100–x)[50ZnO–10B_2O_3–40P_2O_5]·xSb_2O_3$ glasses increases with increasing Sb_2O_3 content. Nevertheless, from the range of obtained ΔC_p values we can classify the studied glasses as typical strong liquids [11].

From the obtained dilatation curves of the studied glasses we have got glass transition temperatures T_g which were by 6–8°C higher than the values obtained from DSC curves. Dilatation softening temperature T_d was usually by 20–30°C above T_g values. Compositional trends in both glass series were similar as the trends in T_g determined from DSC curves. The compositional dependence of thermal expansion coefficient, α, (evaluated in the temperature range of 150–250°C) of the glass samples from the series of $(100–x)[50ZnO–10B_2O_3–40P_2O_5]·xSb_2O_3$ is shown in

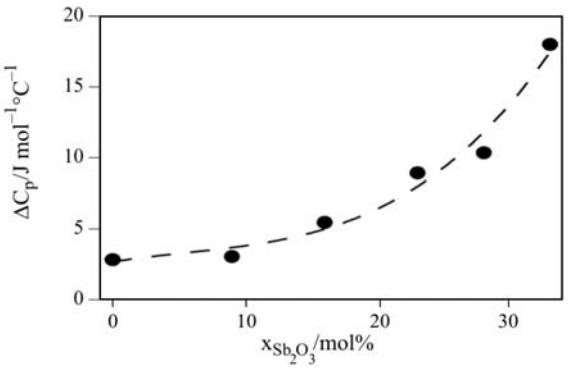

Fig. 5 Changes in heat capacity in the glass transition region for the $(100–x)[50ZnO–10B_2O_3–40P_2O_5]·xSb_2O_3$ glasses

Fig. 3 and that of the glass samples from the series $(100–y)[60ZnO–10B_2O_3–30P_2O_5]\cdot ySb_2O_3$ is shown in Fig. 4. In both compositional series the values of α increase with increasing Sb_2O_3 content. In the first series α increases from 6.6 up to 11 ppm $°C^{-1}$, whereas in the second series α increases from 7.3 to 9.3 ppm $°C^{-1}$.

DSC curves (Figs 1 and 2) show also that all glasses crystallize on heating in the temperature range of 500–622°C. As can be seen from Fig. 1, thermoanalytical curves of glasses with a low Sb_2O_3 content reveal at least 2 crystallization steps, as well as the glasses with a high Sb_2O_3 content. The crystallization temperature T_c in the glasses of the $(100–x)[50ZnO–10B_2O_3–40P_2O_5]\cdot xSb_2O_3$ series decreases with increasing Sb_2O_3 content up to x=23 mol% Sb_2O_3 and remains nearly unchanged (Fig. 3), whereas in the second glass series $(100–y)[60ZnO–10B_2O_3–30P_2O_5]\cdot ySb_2O_3$ T_c reveals a minimum in the glass with y=16.7 mol% Sb_2O_3. The reproducibility in the determination of crystallization temperature is lower than at T_g values. We have observed that measurements of thermoanalytical curves in alumina crucibles gave close T_g values, but substantially lower T_c values (by 40–60°C than in silica crucibles). We assume that the heterogeneous nucleation of crystallization processes take place on the alumina/glass sample contact, which is the reason for the observed lower crystallization temperatures of the studied glasses at the DSC measurements in alumina crucibles.

We have tried to identify the crystallization products using X-ray diffraction. In the parent glass of the composition $50ZnO–10B_2O_3–40P_2O_5$ we found that the first crystallization peak corresponds to the formation of crystalline boron phosphate BPO_4 and the second to the formation of crystalline zinc diphosphate $Zn_2P_2O_7$. With increasing amount of Sb_2O_3 in the studied glasses diffraction lines of antimony orthophosphate $SbPO_4$ can be observed on the X-ray diffraction pattern and the intensity of diffraction lines of $SbPO_4$ increases with increasing Sb_2O_3 content. As some amount of phosphate anions is used for the formation of $SbPO_4$, the ratio of ZnO/P_2O_5 in the remaining composition increases, which results in a decrease in the content of zinc diphosphate $Zn_2P_2O_7$ and an increasing content of zinc orthophosphate $Zn_3(PO_4)_2$ in the crystallization products. In some glass compositions with a high Sb_2O_3 content we have observed in X-ray diffraction patterns also diffraction lines of $Zn(SbO_3)_2$ compound containing Sb^{5+}. As the melting of the studied glasses is carried out in air, it seems that the reactions $Sb^{3+}\leftrightarrow Sb^{5+}$ take place during the melting and cooling glass melt.

Conclusions

This study showed that zinc-borophosphate glasses are able to dissolve a relatively high amount of antimony oxide. The incorporation of Sb_2O_3 into the structural network of both parent zinc borophosphate glasses of the composition $50ZnO–10B_2O_3–40P_2O_5$ and $60ZnO–10B_2O_3–30P_2O_5$ results in a decrease of the glass transition temperature, which shows on the weakening of chemical bonds in the glassy network. The evaluation of strong/fragile character of glass melts showed that the melts of studied glasses belong to strong liquids. An observed increase of fragility of the studied glasses with increasing Sb_2O_3 content is in a good agreement with the weakening of chemical bonds in the glass structure reflected by a decrease in glass transition temperature.

Acknowledgements

The authors are grateful for the financial support from the research project No. 0021627501 of the Ministry of Education of Czech Republic and to the Grant Agency of the Czech Republic (Grant No. 104/07/0315).

References

1 T. M. Alam and R. K. Brow, J. Non-Cryst. Solids, 223 (1998) 1.
2 R. K. Brow and D. R. Tallant, J. Non-Cryst. Solids, 222 (1997) 396.
3 D. F. Ushakov, N. F. Baskova and Yu. P. Tarlakov, Fiz. Khim. Stekla, 1 (1975) 151.
4 J. M. Clinton and W. W. Coffeen, Ceram. Bull., 63 (1984) 1401.
5 R. K. Brow, J. Non-Cryst. Solids, 194 (1996) 267.
6 L. Koudelka and P. Mošner, Mater. Lett., 42 (2000) 194.
7 P. Mošner and L. Koudelka, Sci. Pap. Univ. Pardubice, Ser. A, 4 (1988) 75.
8 L. Koudelka, P. Mošner, J. Pospíšil, P. Montagne and G. Palavit, J. Solid State Chem., 178 (2005) 1837.
9 J. Pospíšil, P. Mošner and L. Koudelka, J. Therm. Anal. Cal., 84 (2006) 479
10 L. Koudelka, J. Šubčík, P. Mošner, L. Montagne and L. Delevoye, J. Non-Cryst. Solids, (in print).
11 D. Zhu, C. S. Ray, W. Zhou and D. E. Day, J. Non-Cryst. Solids, 319 (2003) 247.

Received: March 21, 2007
Accepted: April 18, 2007
OnlineFirst: June 28, 2007

DOI: 10.1007/s10973-007-8457-1